

Far field characterization of diffracting circular apertures

Christian Obermüller and Khaled Karrai^{a)}

Walter Schottky Institut, Technische Universität München, 85748 Garching, Germany

(Received 3 July 1995; accepted for publication 22 September 1995)

The far field angular intensity distribution $I(\theta)$ of the $\lambda=633$ nm radiation transmitted through diffracting circular apertures is measured for diameters ranging between 60 and 500 nm. The circular apertures are located at the apex of aluminum coated tapered optical fiber tips. $I(\theta)$ depends sensitively on the aperture diameters down to $\lambda/6$. This property is used to determine the optical aperture size of metal coated tapered optical fiber tips used for near field scanning optical microscopy. © 1995 American Institute of Physics.

The spatial lateral resolution of far field optical microscopy is fundamentally limited to details with sizes of the order of the wavelength λ . This basic diffraction barrier is overcome in near field scanning optical microscopy (NSOM). In this mode of operation a sample is positioned in the near field vicinity of a light source of size typically much smaller than λ . Although the principles of NSOM have been proposed early in this century¹ and demonstrated for radiation in the visible about a decade ago,² it has become a useful art of microscopy only very recently. A breakthrough was made in 1991 by Betzig and Trautman when they produced a subwavelength sized circular aperture at the apex of metal coated tapered optical fiber tips.³ Visible laser radiation can be ported in the optical fiber down to the aperture vicinity with such a great efficiency that aperture photon throughputs in the nanowatt range became possible. Such optical apertures, used as a local light source, can be made with diameters $2a$ as small as 40 nm. In NSOM, the lateral spatial resolution is no longer limited to λ but is rather of the order of $2a$. Such resolution can be obtained when the object is placed within the depth of field of the local source. For subwavelength sized apertures, this depth of field is also of the order of $2a$. It appears that a proper interpretation of NSOM imaging, depends critically on the knowledge of a , which is generally speaking the typical light confinement radius of the local source. We propose in this letter a simple and convenient far field optical characterization method which allows us to determine apertures radii down to $\lambda/6$.

The idea behind the present method is based on the following observation. The angular far field intensity distribution of a monochromatic radiation transmitted through a diffracting aperture depends on a . Strictly speaking, knowing λ , it is possible to infer the aperture size by measuring the angular intensity distribution of the diffracted field. The question is what is the dependence and the sensitivity of this angular distribution to a . In this work, we are experimentally addressing this problem for the particular case for which the aperture is formed at the apex of a metal coated tapered optical fiber tip. The answer was approached theoretically in the idealized case for which the circular aperture of radius “ a ” lies in an infinitely thin two-dimensional perfectly conducting screen. This idealized case has been treated rigor-

ously and formally by Meixner and Andrejewski.⁴ The exact solution of this apparently simple problem is the result of tedious and complicated calculations and is expressed in an intricate series of spheroidal functions which rate of convergence depends on ka , where $k=2\pi/\lambda$ is the wave vector. For uniform electromagnetic fields normally incident on the screen, the limiting case of large holes (i.e., $ka \gg 1$) reduces to the result of Kirchhoff's scalar theory. In this limiting case, the normalized angular dependence of the far field intensity is $I_{\text{Kir}}(\theta)=[2J_1(\xi)/\xi]^2$, where J_1 the Bessel function of the first kind and $\xi=(ka)\sin(\theta)$. The angle θ spans the direction normal to the aperture plane and the direction pointing to the detector.

Another limiting case of practical importance for NSOM is the small aperture radius limit (i.e., $ka \ll 1$). This problem was addressed by Bethe⁵ in 1944. Although Bethe's solution proved wrong in the near field range,⁶ its far field limit is correct.⁷ The main result of Bethe's theory is that in the limit of $ka \ll 1$, the far field radiation of the aperture is identical to that of a combination of two radiating dipoles located at the center of the aperture.^{5,7} One of them is an in-plane magnetic dipole \mathbf{M} antiparallel to the magnetic field component \mathbf{H}_0 of the radiation falling on the screen. The other one is an electric dipole \mathbf{P} directed along $\mathbf{E}_{0\perp}$ the incoming radiation electric field component perpendicular to the screen. In particular for the case of a plane wave at normal incidence, $\mathbf{E}_{0\perp}=\mathbf{P}=0$. The radiation reduces then to that of a single magnetic radiating dipole, leading to $\mathbf{I}_{\text{Bethe}}^{\parallel}(\theta)=\cos^2(\theta)$ when the detector is scanned in a plane containing \mathbf{M} , and to $\mathbf{I}_{\text{Bethe}}^{\perp}=1$ when the detector is scanned in the plane perpendicular to \mathbf{M} . At this point we see that \mathbf{I}_{Kir} (i.e., $ka \gg 1$) is dramatically different from $\mathbf{I}_{\text{Bethe}}$ (i.e., $ka \ll 1$). One striking difference is that $\mathbf{I}_{\text{Bethe}}$ is polarization dependent while \mathbf{I}_{Kir} is not. The quantitative difference between the two limiting cases is well illustrated when expressed in terms of $2\theta_{1/2}$ the full width at half-maximum (FWHM) of $\mathbf{I}(\theta)$. This quantity is obviously irrelevant for $\mathbf{I}_{\text{Bethe}}^{\perp}=1$. For the $ka \ll 1$ limit, the FWHM is obtained by equating $\mathbf{I}_{\text{Bethe}}^{\parallel}(\theta_{1/2})=\cos^2(\theta_{1/2})=1/2$ leading to $2\theta_{1/2}=90^\circ$ which does not depend on ka . On the other hand, in the $ka \gg 1$ limit, the FWHM is given by solving $\mathbf{I}_{\text{Kir}}(\theta_{1/2})=1/2$ leading to $2\theta_{1/2}=2\arcsin(1.6163/ka) \sim 3.233/ka$. The expected qualitative dependence of the FWHM on ka , is that $2\theta_{1/2}$ should increase with reducing ka until it reaches a saturation at 90° for $ka=0$. The exact de-

^{a)}Electronic mail: kkarrai@cip.physik.tu-muenchen.de

pendence of $2\theta_{1/2}$ on ka could be, in principle, numerically determined using the results of Ref. 4. Solving the exact problem for the case of a circular aperture in a flat metal screen, although of qualitative interest, fails as we will see it to describe quantitatively the far field angular distribution of a tapered optical fiber tip aperture radiation emitted through apertures at the apex of metal coated tapered tips when ka ranges from 0.5 to 2.

The geometry of the present measurement is defined as follows. The tip axis is aligned along Z so that the circular aperture lies in the plane XY . The electric field polarization of the outgoing radiation lies in the plane XZ . We define the following angles θ and Φ in spherical coordinates. As previously defined, θ determines the angle between the tip axis Z and the detector direction. $\theta=0$ represents the situation in which the detector faces the tip aperture. At $\theta=90^\circ$ the detector lies in the plane XY of the aperture. Φ defines the angle formed by the plane in which the detector is scanned and XZ the plane of the electric field polarization of the transmitted radiation. In the present experimental setup we have used a semiconducting photodetector diode scanned along a circular path having the tip aperture for center and a radius of $R=5$ cm. The detector optical path is free for θ ranging between -165° and 165° . The angular resolution in $I(\theta)$ is adjustable from 0.3° to 8° depending on the detector numerical aperture. A linear polarizer used as an analyzer was placed just in front of the detector. The linearly polarized light of the $\lambda=633$ nm HeNe laser line was launched into the optical fiber with an intensity of 1 mW. The outgoing intensity through the aperture ranged from 1 to 100 nW for aperture sizes ranging from $2a=60$ to 200 nm and was in the microwatt range for larger apertures. The tips were found to preserve the linear polarization of the incoming light to better than 97% for the whole range of the aperture diameter. The whole angular measurement apparatus was placed in a dark enclosure in order to avoid photon signal extrinsic to the aperture transmission. In particular, the fiber was inserted in an opaque tube so that the detector would not be exposed to parasitic light scattering occurring within the fiber. The tapered metal coated fiber tips used for this work were prepared by melting and pulling monomode optical fibers with a $3.2\text{ }\mu\text{m}$ core diameter and $125\text{ }\mu\text{m}$ cladding according to the technique outlined in Ref. 3. For this purpose, we used a commercial pipette puller fitted with a 10 W CO_2 laser. A 150 nm thin aluminum film is evaporated on the sides of the tips leaving their apex unobstructed as shown in Fig. 1.

We have performed two types of $I(\theta)$ measurement scans. The case $\Phi=0$, where the detector travels in the plane of polarization XZ , and the case $\Phi=90^\circ$, in which the detector travels in the plane XZ perpendicular to the plane of polarization. The results for $\Phi=0$ are shown in Fig. 2. The narrowest $I(\theta)$ distribution was obtained using a flat, cleaved optical fiber (i.e., without a tip). Its FWHM is $2\theta_{1/2}=5.36^\circ$ defined somewhat by the core radius of the fiber. In this case, as expected, $I(\theta)$ is maximum when the detector faces the aperture (i.e., $\theta=0$) and is perfectly fitted with a Gaussian function. The signal level falls to the noise background level when $|\theta|$ exceeds 15° . When the aperture diameter is reduced

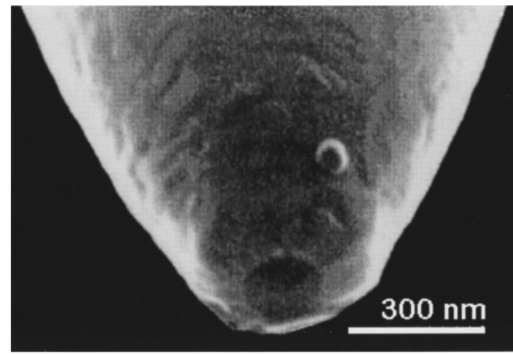


FIG. 1. A scanning electron micrograph showing a 161 nm circular aperture at the apex of a tapered aluminum coated optical fiber tip. The aluminum coating is 120 nm thick, the tip taper angle is 32° . Such an aperture allows a photon throughout up to 80 nW (for $\lambda=633$) and maintains linear polarization up to 97%.

to 380 nm, $I(\theta)$ becomes much broader. Although its shape remains Gaussian, the $I(\theta)$ peak rides in this case on a constant photon intensity background corresponding to 6.6% of the maximum signal. We find it remarkable that a finite photosignal is measured for $|\theta|>90^\circ$, which corresponds to backward scattered light transmitted through the aperture. When the aperture diameter is further reduced, $I(\theta)$ gets broader and the background signal larger. In Fig. 2 we have displayed the result for the smallest aperture of 60 nm diameter. In this case, the background signal is 38% of $I(0)$ showing that a large proportion of the photon intensity is backward diffracted. In Fig. 2, Bethe's prediction is $I_{\text{Bethe}}^\perp=1$ for $-90^\circ\leq\theta\leq90^\circ$, which is in complete discrepancy with the present data.

As shown in Fig. 3, measurements were also carried for $\Phi=90^\circ$. The cleaved fiber aperture was measured to have the same $I(\theta)$ as in Fig. 2, as expected from Kirchhoff's diffraction theory. As the aperture size was made smaller, $I(\theta)$ was found to be different from the case $\Phi=0$. In particular, very little background photon signal was found. For the smallest tip diameter of 60 nm, a minimum was found at $\theta=\pm120^\circ$. This result was found reproducible for many tips of the same size. It is important, however, to point out that the symmetry and shape of $I(\theta)$ is very sensitive on the metal film quality.

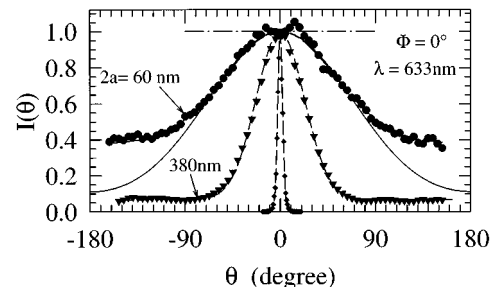


FIG. 2. Normalized angular dependence of the transmitted intensity $I(\theta)$ measured for aperture diameters of $2a=60$ nm ($ka=0.30$), $2a=380$ nm ($ka=1.89$), and $2a=3.2\text{ }\mu\text{m}$ ($ka=15.9$). The detector is scanned in the plane of the polarization ($\Phi=0$). The dash-dotted line spanning -90° to 90° corresponds to Bethe's theory. The dashed lines corresponds to the best Gaussian fit. The full line corresponds to the case of magnetic and electric radiating dipoles of strength 2 and 1, respectively, and placed perpendicular to each other in the plane of the aperture.

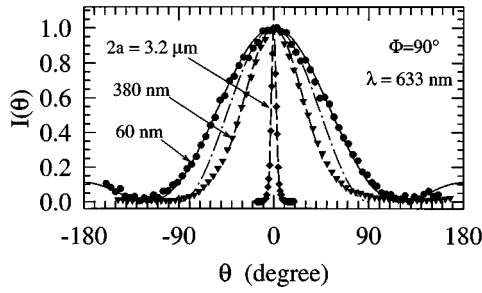


FIG. 3. Same as Fig. 2 but in this case, the detector is scanned in the plane XY perpendicular to that XZ of the light polarization (i.e., $\Phi=90^\circ$). The dashed-dotted line correspond to Bethe's prediction.

Any undesired light leakage produces interferences patterns easily detected in $I(\theta)$. Here again, Bethe's theory fails to describe the present data since it predicts $I_{\text{Bethe}}^{\parallel}(\theta) = \cos^2(\theta)$. Inspired by Bethe's far field equivalence existing between small apertures and a combination of two dipoles, we have tried to find the best linear combination for \mathbf{M} and \mathbf{P} in order to fit the 60 nm aperture data. To our surprise, we found that the fit is perfect for a choice of \mathbf{M} and \mathbf{P} proportional in magnitude to that of Bethe but with \mathbf{P} lying in the XY plane aperture being parallel to \mathbf{E}_0 the field of the radiation in the fiber before the aperture. \mathbf{M} is parallel to the magnetic field component \mathbf{H}_0 of the radiation before the tip aperture. The result is

$$\mathbf{P} = [a^3/(3\pi)]\alpha\mathbf{E}_0 \text{ and } \mathbf{M} = 2[a^3/(3\pi)](\mu_0 c)\alpha\mathbf{H}_0, \quad (1)$$

where a is the aperture radius and α is an unknown proportionality factor. The corresponding intensity $I(\theta)$, given by the Poynting vector's amplitude normalized in units of solid angle is

$$\mathbf{S} = \alpha^2/(36\pi^3)(a/R)^2(ka)^4[2(\mu_0 c)\boldsymbol{\mu} \times \mathbf{H}_0 + \mathbf{u} \times (\mathbf{u} \times \mathbf{E}_0)]^2 \cdot \mathbf{u}, \quad (2)$$

where \mathbf{u} is the unit vector pointing from the tip to the detector. $I(\theta)$ is given by the amplitude of \mathbf{S} normalized to its maximum. Specializing to the case $\Phi=90^\circ$, Eq. (2) leads to $I(\theta) = [(2 \cos \theta + 1)/3]^2$ which is precisely the full line going through the 60 nm aperture data points in Fig. 3. For the scan geometry $\Phi=0$, Eq. (2) gives $I(\theta) = [(\cos \theta + 2)/3]^2$ also shown in Fig. 2. In this case the data are well reproduced only in the $-75^\circ \leq \theta \leq 75^\circ$. It was not possible to find a combination of two dipoles simultaneously satisfying the $\Phi=0$ and $\Phi=90^\circ$ data scan.

Since in the case of $\Phi=90^\circ$ the $I(\theta)$ peak rides on a zero signal background, it makes sense to use the FWHM as a parameter characterizing the distribution $I(\theta)$. In Fig. 4 this FWHM as a function of the tip aperture, determined inde-

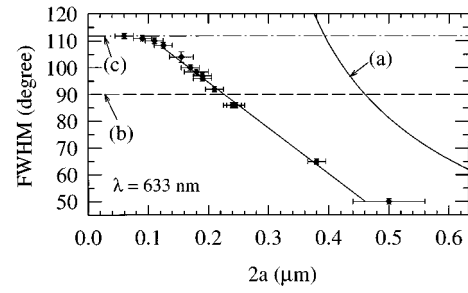


FIG. 4. Full width at half-maximum of the angular distribution of $I(\theta)$ the far field intensity as a function of the aperture diameter. All measurements were carried out with polarized light and $\Phi=90^\circ$. These data show that far field measurements allow us to reliably determine the aperture size down to $\lambda/5$; (a) is obtained using Kirchoff's theory, (b) is the small aperture limit theory of Bethe, and (c) is given by the simple model discussed in the text. The line is the best linear fit for tips with diameters larger than 100 nm.

pendently from scanning electron micrographs, was plotted. The data shows that from such rather simple far field measurements, it is possible to determine, with a reasonable accuracy, the aperture diameter at the tip apex of a metal coated tapered tip down to about $\lambda/6$. This is particularly attractive since one can obtain this way direct information about the optical size of the aperture. Such a method, however, proves to be not sensitive enough when the aperture diameter gets smaller than $\lambda/6$. This puts the limits of $2a_{\min} = 106$ nm when the HeNe $\lambda=633$ nm laser line is used and $2a_{\min} = 76$ nm for the $\lambda=458$ nm ion argon laser line. The intensity of the photon background seen in Fig. 2 for $\phi=0$ seems to follow a similar dependence.

The discrepancy that exists between the idealized flat screen model and the present results for tapered tips is expected since the geometry of the metallic boundary conditions play a determinant role in the spatial distribution of the electromagnetic waves transmitted through the tip apertures.⁵⁻⁸ During the writing of this letter we have learned that Novotny *et al.* have recently numerically modeled such a distribution for a realistic tip shape.⁹

The authors gratefully acknowledge discussions with R. D. Grober and L. Novotny. This work was supported by the Deutsche Forschungsgemeinschaft vis SFB 348. K. Karrai was supported in part by the A. von Humboldt Foundation.

¹E. H. Synge, Philos. Mag. **6**, 356 (1928).

²D. W. Pohl, W. Denk, and M. Lanz, Appl. Phys. Lett. **44**, 651 (1984).

³E. Betzig, J. K. Trautman, T. D. Harris J. S. Weiner, and R. L. Kostelak, Science **251**, 1468 (1991).

⁴J. Meixner and W. Andrewjeski, Ann. Phys. **7**, 157 (1950).

⁵H. A. Bethe, Phys. Rev. **66**, 163 (1944).

⁶C. J. Bouwkamp, Philips Res. Rep. **5**, 401 (1950).

⁷C. J. Bouwkamp, Rep. Prog. Phys. **17**, 35 (1954).

⁸Y. Leviatan, J. Appl. Phys. **60**, 1577 (1986).

⁹L. Novotny, D. W. Pohl, and B. Hecht, Opt. Lett. **20**, 970 (1995).